Available online at www.sciencedirect.com
ScienceDirect
Trans. Nonferrous Met. Soc. China 23(2013) 3553−3560
Transactions of Nonferrous Metals Society of China
www.tnmsc.cn

Intermetallic phase evolution of 5059 aluminum alloy during homogenization

Hai-chun JIANG[1,2], Ling-ying YE[1,2], Xin-ming ZHANG[1,2], Gang GU[1,2], Pan ZHANG[1,2], Yu-long WU[1,2]

1. School of Materials Science and Engineering, Central South University, Changsha 410083, China;
2. Key Laboratory of Nonferrous Materials Science and Engineering of Ministry of Education, Central South University, Changsha 410083, China

Received 20 July 2013; accepted 25 October 2013

Abstract: Intermetallic phase evolution of 5059 aluminum alloy during homogenization was investigated by means of optical microscopy (OM), scanning electron microscopy (SEM), transmission electron microscopy (TEM), energy dispersive spectrometry (EDS), differential scanning calorimetry (DSC) and X-ray diffraction analysis (XRD). The results show that severe dendritic segregation exists in as-cast alloy. The dissolvable intermetallic phases in as-cast alloy consist of Zn- and Cu-rich non-equilibrium β (Al_3Mg_2) phase, Fe-rich eutectic Al_6Mn phase and equilibrium Mg_2Si phase. During the homogenization, Zn- and Cu-rich non-equilibrium β (Al_3Mg_2) phase, Fe-rich eutectic Al_6Mn phase and equilibrium Mg_2Si gradually dissolve into matrix. Fine dispersed β(Al_3Mg_2) particles and rod-shaped Al_6Mn particles form in the Al matrix after homogenization. The proper homogenization processing is at 450 °C for 24 h, which is consistent with the results of homogenizing kinetic analysis.
Key words: intermetallic phase; 5059 aluminum alloy; homogenization; microstructure; evolution

1 Introduction

5059 aluminum alloy, with medium to high strength, better corrosion resistance, excellent formability and good recycling ability, possesses great application potential in the automotive, marine, construction and aerospace industries [1]. Although the main strengthening effects of 5059 aluminum alloy come from solid solution strengthening and strain hardening. A number of alloying elements are introduced to improve its other properties, such as introducing alloying elements Mn, Cr to ameliorate the mechanical property, adding alloying element Zn to improve the corrosion resistance and the weldability with the addition of Zr element [2−5].

Because of the heavy alloying and the fast cooling rate during the conventional DC casting, quantities of intermetallic phases form in the cast alloy. In order to obtain good processing properties and service performance, the as-cast alloys should be homogenized before subsequent processing. The homogenization temperature and time play a very important role in the dissolution of the residual phases during the homogenization. Usually, the residual coarse particles of Fe- or Zn- and Cu-rich phases will result in a decrease of toughness and strength, and deteriorate subsequent deformation processing [6−11].

Despite several researches have been carried out on the Al−Mg (5000 series) alloys [12−16], there is still a lack of detailed investigation of the effects of homogenization on the microstructure evolution of the 5059 aluminum alloy. As the type and the intrinsic character of the intermetallic phases will vary in different alloys or in one alloy at different solidification and homogenization conditions. So, it is important to investigate the evolution of intermetallic phases and to develop a proper homogenization process for 5059 aluminum alloy. Besides, the homogenization kinetic equation of 5059 aluminum alloy was also set up to proving the result.

2 Experimental

The experimental material 5059 aluminum alloy was prepared with industrial pure Al, Mg, Zn, Cu and Al−Mn, Al−Cr, Al−Zr master alloy in an electrical resistance furnace. After the grain refinement with Al–Ti–B (5:1 in mass ratio) master alloy, the homogeneous liquid was cast in a steel mould. The

Foundation item: Project (2012CB619501) supported by the National Basic Research Program of China
Corresponding author: Ling-ying YE; Tel: +86-13607435545; E-mail: 30575421@qq.com
DOI: 10.1016/S1003-6326(13)62900-3

normal chemical compositions of 5059 aluminum alloy are listed in Table 1.

Table 1 Nominal chemical composition of different alloys (mass fraction, %)

Mg	Mn	Zn	Cr	Zr	Ti	Cu	Al
5.8	1.00	0.80	0.15	0.15	0.05	0.20	Bal.

All specimens for homogenization were taken from the center of the ingot with the dimensions of 10 mm× 10 mm × 10 mm. The specimens were homogenized at 420, 430, 440, 450, and 460 °C for 8, 16, 24 and 36 h, respectively.

The samples for observation were prepared by standard metallographic procedures and etched with Keller reagent (2 mL HF, 3 mL HCl, 5 mL HNO_3 and 190 mL water). Then the samples were observed using optical microscope (OM) and scanning electron microscope (SEM). The color and shape of phases were used for quantitative analysis. In optical micrographs, the Al matrix appears grey, whereas the intermetallic phases are white or light grey. The volume fraction of the intermetallic phases was measured using the image analysis software Image-pro Plus 5.0. The area fraction was assumed to be equivalent to the volume fraction.

The composition of the large intermetallic particles was measured on an energy dispersive X-ray analyzer (EDS). High magnification observations were carried out on a FEI TECNAI G2−20 type transmission electron microscope (TEM) equipped with Oxford INCAX-Sights energy dispersive spectroscope. The TEM foils were prepared by twin-jet thinning electrolytically in a solution of 30% nitric acid and 70% methanol at −25 °C. And differential scanning calorimetry DSC analyses were conducted using a SDT−Q600 differential scanning calorimeter to decide the overburnt temperature at a constant heating rate of 10 °C/min from 25 °C to 600 °C and the standard sample was pure Al.

3 Results and discussion

3.1 As-cast microstructure

The as-cast microstructures are shown in Fig. 1. It consists of α(Al) and many kinds of intermetallic phases (Fig. 1(a)). They were identified by a combination of morphology (Fig. 1) and composition analysis (Table 2). The continuous grey secondary phase *A* shown in Fig. 1(a) is identified as some Zn-, Cu-contained $\beta(Al_3Mg_2)$ phase. Little white phases *B* and *D* are Al_6Mn, and some contain small amount of Fe. The dark irregular phase is AlMgSi. The EDX results are shown in Table 2. There are two kinds of primary $FeMnAl_6$ constituent phases: one is present as a discrete blocky with size of 10−40 μm, and the other is present as a skeleton shape

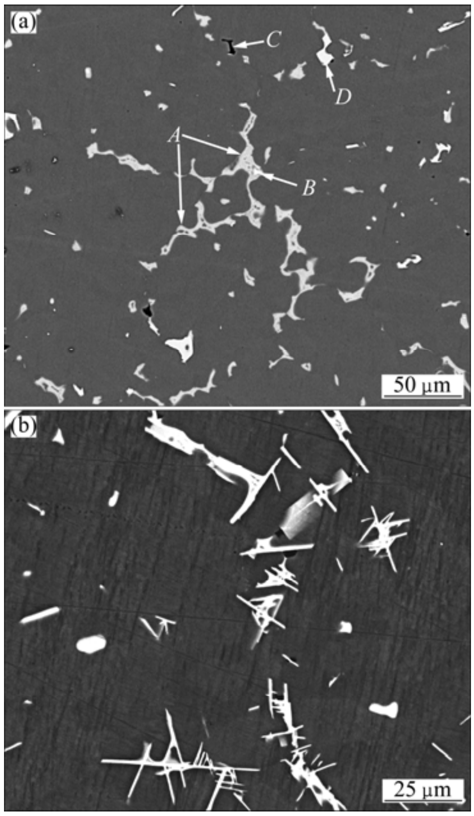

Fig. 1 SEM images of as-cast 5059 alloy

Table 2 Chemical composition of intermetallic compounds at grain boundary in Fig. 1

Phase	x(Mg)/ %	x(Mn)/ %	x(Fe)/ %	x(Zn)/ %	x(Cu)/ %	x(Si)/ %	x(Al)/ %
A	32.08	−	−	05.09	02.55	−	60.27
B	06.17	10.88	03.42	−	−	−	79.53
C	25.16	−	−	−	01.23	08.97	64.64
D	−	09.79	05.03	−	−	−	85.78

and there is a continuous network at interdendritic regions (Fig. 1(b)).

Figure 2 shows the scanning electron microstructure and the main elements Mg, Mn and Zn distribution in as-cast alloy. The main elements Mg, Mn and Zn are largely enriched at grain boundaries, and the concentration of the elements decreases from grain boundary to inside. And the segregation degree is Mg>Zn>Mn.

Therefore, the homogenization treatment is required to eliminate severe dendritic segregation in the as-cast alloy. Generally, the relationship between diffusion coefficient and the temperature can be described as

$$D=D_0\exp\left(-\frac{Q}{RT}\right) \quad (1)$$

where D_0 is the diffusion coefficient, *R* is the mole gas constant, *Q* is the diffusion activation energy and *T* is the

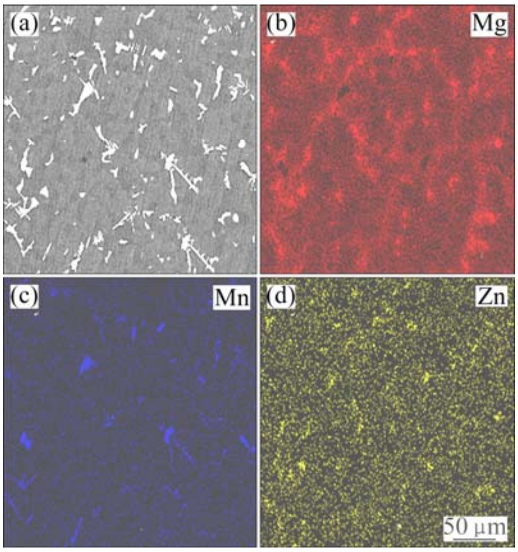

Fig. 2 Scanning electron microstructure and main elements distribution in as-cast alloy: (a) Backscattered electron image; (b) Element distribution of Mg; (c) Element distribution of Mn; (d) Element distribution of Zn

thermodynamic temperature. It can be seen from Eq. (1) that the higher the temperature, the larger the diffusion coefficient, which makes it easier to eliminate the dendritic segregation in the as-cast alloy. However, higher temperature increases the possibility of overburning of the alloy. Thus, it is highly necessary to optimize the homogenization temperature.

3.2 DSC analysis of as-cast and homogenized alloy

DSC curves of as-cast and homogenized 5059 aluminum alloy are shown in Fig. 3. The area under a given DSC peak relates to the phase volume fraction, and is calculated qualitatively by its enthalpy value. The peak temperature of a given reaction is dependent on the phase composition under the same condition. The temperatures and enthalpy values, corresponding to endothermic dissolution peaks obtained from DSC curves in Fig. 3, are shown in Fig. 4.

Only one endothermic peak, sited at 459.9 °C, is observed in the as-cast alloy. After homogenizing in different processes, the endothermic peak still exists, but the enthalpy value corresponding to this peak decreases. Therefore, it can be inferred that the low melting point intermetallic phase melt at 459.9 °C. So, the upper limit temperature for homogenization is 459.9 °C. The enthalpy value corresponding to the endothermic peak gradually decreases with the increasing of the homogenization temperature or the prolonging of the holding time. It might be corresponding to the dissolution of some non-equilibrium phases during homogenization.

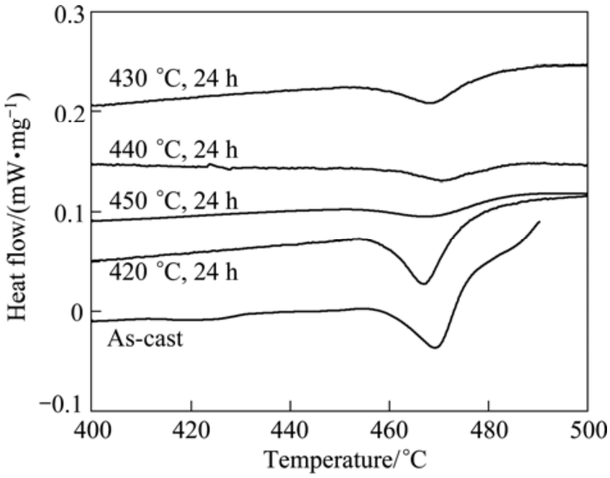

Fig. 3 DSC curves of specimens as-cast and homogenized at different temperatures and time

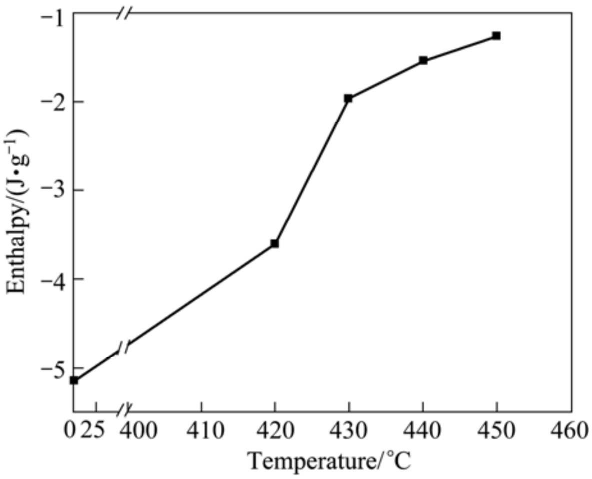

Fig. 4 Temperatures and enthalpy values corresponding to endothermic peaks

3.3 Microstructure of homogenized alloy

Figure 5 shows the optical microstructure of 5059 aluminum alloy homogenized at different temperatures for 24 h. It suggests that the microstructure of the alloy is determined by the homogenization temperature. The volume fraction of the residual phases is significantly reduced with the increase of the homogenization temperature, the grain boundaries become thin and the distribution of the secondary phases along the grain boundaries become discontinuous. When the specimen is homogenized at 450 °C for 24 h, the dendritic network structure disappears and most residual phases spread homogeneously in the matrix (Fig. 5(d)). But when the temperature increases to 460 °C, the specimen is slightly overburnt because of the presence of the melting compounds both in the grain boundaries and triple conjunctions (Fig. 5(e)). This indicates that the upper temperature limit for homogenization is 460 °C.

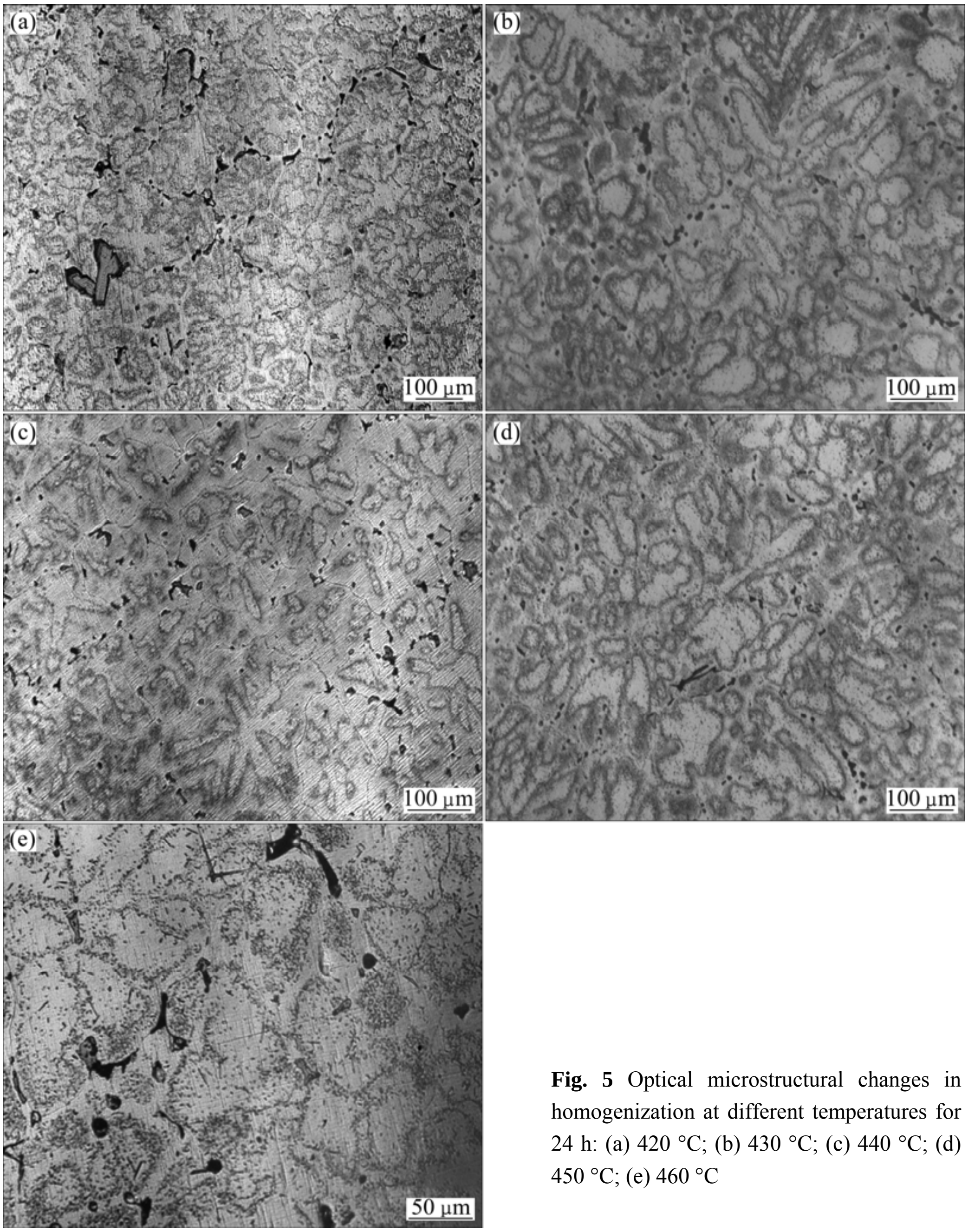

Fig. 5 Optical microstructural changes in homogenization at different temperatures for 24 h: (a) 420 °C; (b) 430 °C; (c) 440 °C; (d) 450 °C; (e) 460 °C

Figure 6 presents the SEM images of 5059 aluminum alloy homogenized at 450 °C for different time. It reveals that by prolonging the holding time, the dendritic-network structure reduces the volume fraction. And the massive residual phases become small and sparse. When the specimen is homogenized for 24 h, the secondary phases are almost dissolved into the matrix (Fig. 6(c)). With further prolonging the holding time, no obvious secondary phase dissolution is observed (Fig. 6(d)).

Figures 7 and 8 give the transformation rules of volume fraction of the intermetallic phases with the homogenization temperature and the holding time respectively. With the increasing of the homogenization temperature or the prolonging of the holding time, the volume fraction of the intermetallic phases declines gradually. When the specimen is homogenized at 450 °C for 24 h, the volume fraction of the intermetallic phases gets the smallest value. As a result, the suitable homogenization treatment for 5059 alloy is at 450 °C for 24 h.

3.4 Evolution of intermetallic phases during homogenization

SEM and TEM images of homogenized alloy are shown in Fig. 9. After homogenization, the dendritic microstructure of the as-cast alloy disappeared. Fine homogeneously dispersed dispersoids precipitated in the

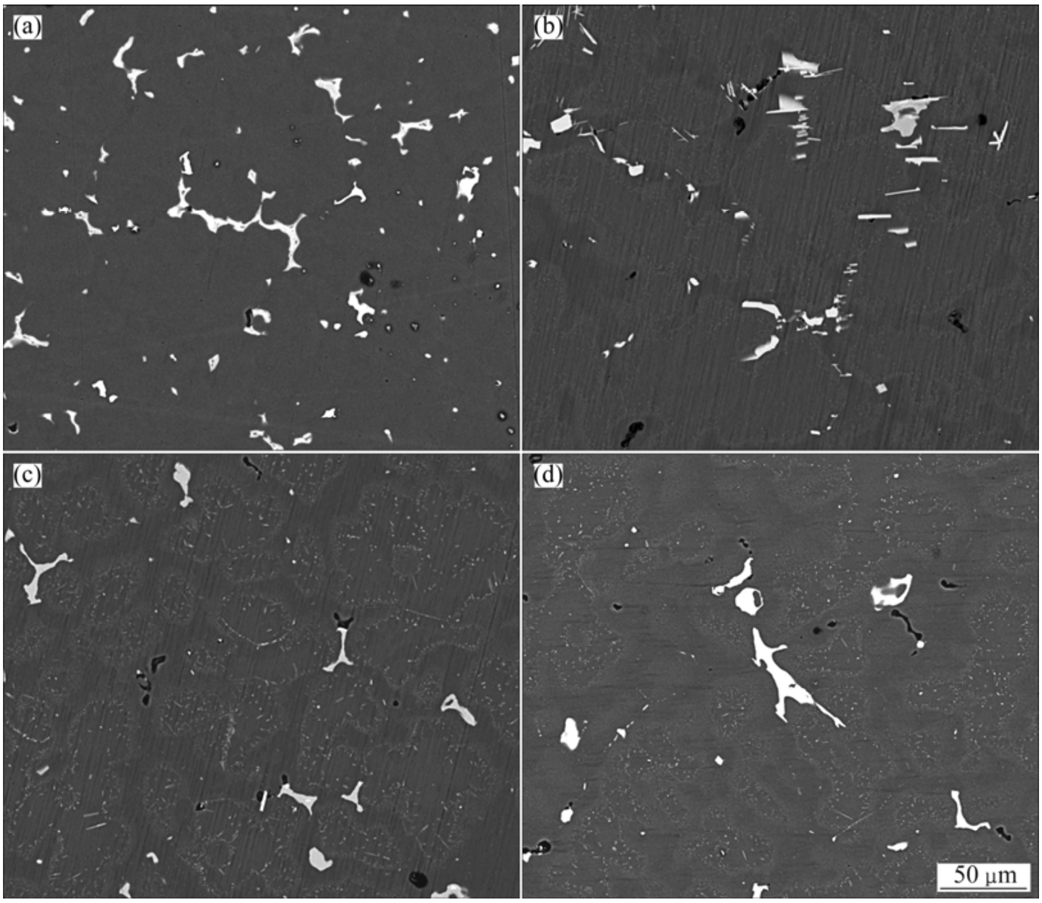

Fig. 6 SEM images of 5059 aluminum alloy homogenized at 450 °C for different time: (a) 8 h; (b) 16 h; (c) 24 h; (d) 36 h

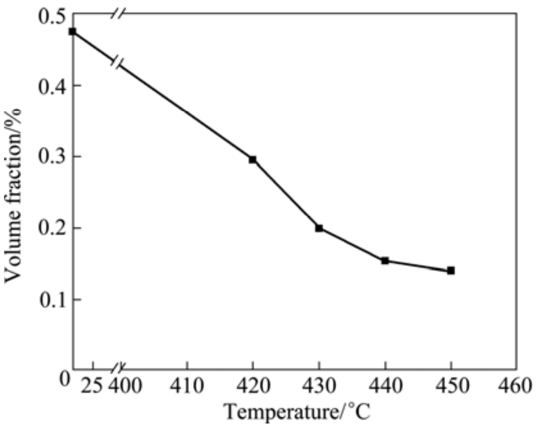

Fig. 7 Volume fraction of intermetallic phases at different homogenization temperatures

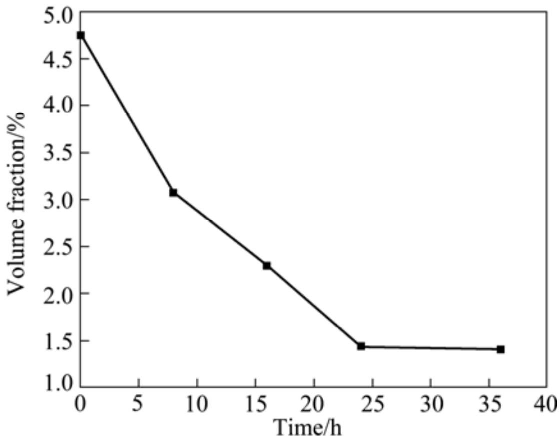

Fig. 8 Volume fraction of intermetallic phases homogenized at 450 °C for different time

aluminum matrix. The compositions of the precipitated phases were determined by EDS and the results are shown in Fig. 10. The cubic particles are AlMgZn compounds and the rod-like particles are AlMn compounds.

3.5 Homogenization kinetic analysis

It can be seen that the distribution of the main elements along interdendritic region varies periodically from Fig. 2. Therefore, the studies on diffusion law along interdendritic region are important to the investigations of elements distribution during homogenization.

According to SHEWMAN [17], the initial concentration of the elements along the interdendritic region can be approached by Fourier series components in a cosine function:

$$c(x)=\overline{c}+A_0\cos\frac{2\pi x}{L} \tag{2}$$

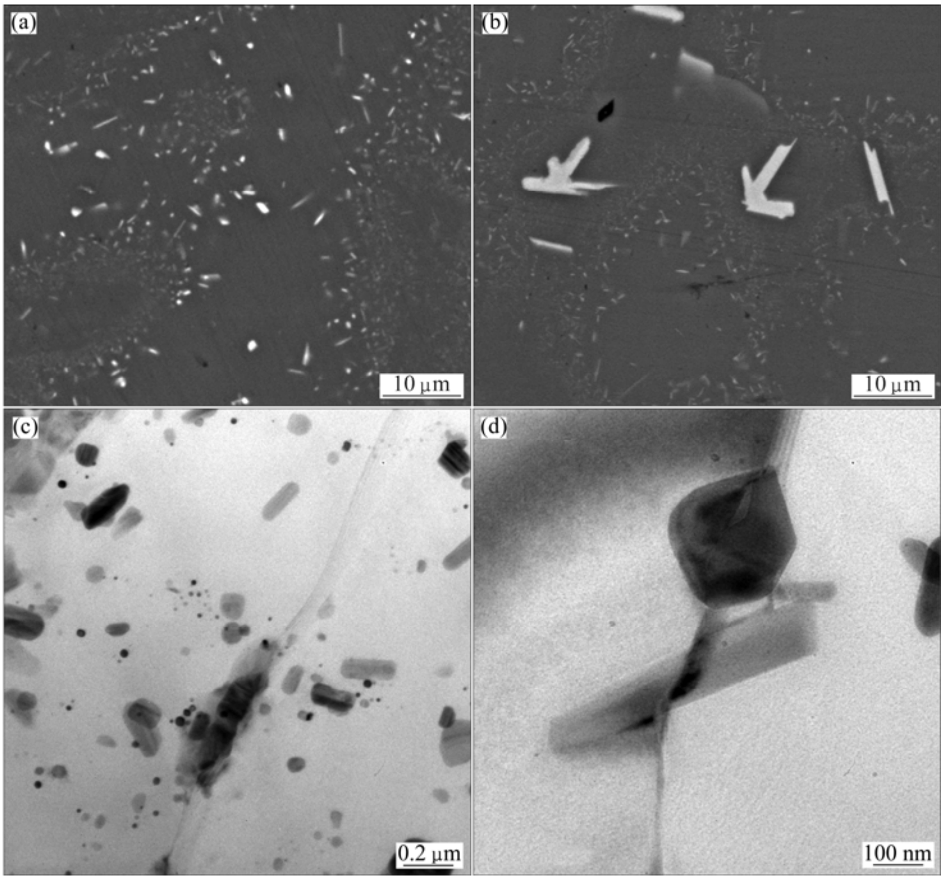

Fig. 9 SEM (a, b) and TEM (c, d) images of homogenized alloy: (a), (c) AlMgZn compounds; (b), (d) AlMn compounds

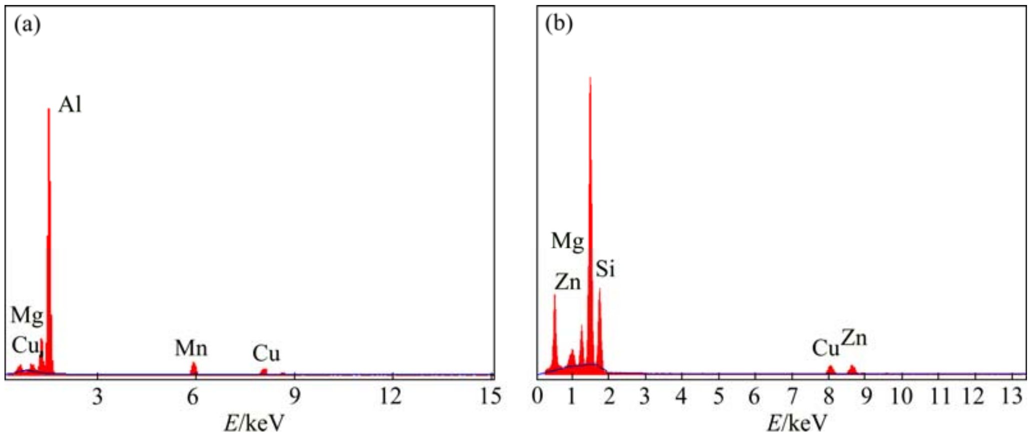

Fig. 10 EDS spectra of precipitated dispersoids: (a) Cubic particle AlMgZn; (b) Rod-like particle AlMn

where $\bar{c}$ is the average concentration of the element, L is the interdendritic spacing and A_0 is the initial amplitude of the composition segregation.

Combining with the Fick's law and assuming that the element distribution is homogeneous when the composition segregation amplitude is reduced to 1%, the homogenization kinetic equation could be obtained:

$$\frac{1}{T}=\frac{R}{Q}\ln\left(\frac{4\pi^2 D_0 t}{4.6L^2}\right) \tag{3}$$

According to the homogenization kinetic equation, if the parameters of as-cast microstructure are given, the homogenization kinetic curves can be obtained. From Ref. [18], it can be concluded that the diffusion coefficient of Mn is much lower than that of Mg or Zn at the same temperature. So, the homogenization process is believed to be controlled by the diffusion of Mn. By substituting of D_0(Mn)=2.2×10^{-5} m^2/s, Q(Mn)=120.5 kJ/mol and R=8.314 J/(mol·K) into Eq. (3), the homogenization kinetic curves of 5059 aluminum alloy can be obtained. The average interdendritic spacing (L) is 129.74 μm based on the quantitative metallographic analysis. According to the homogenization kinetic curve shown in Fig. 11, at the optimized temperatures of 450 °C, the corresponding homogenization time is 18.9 h. This is in good accordance with the experimental result. The scanning electron microstructure and the main elements Mg, Mn and Zn distribution in homogenized alloy are shown in the Fig. 12.

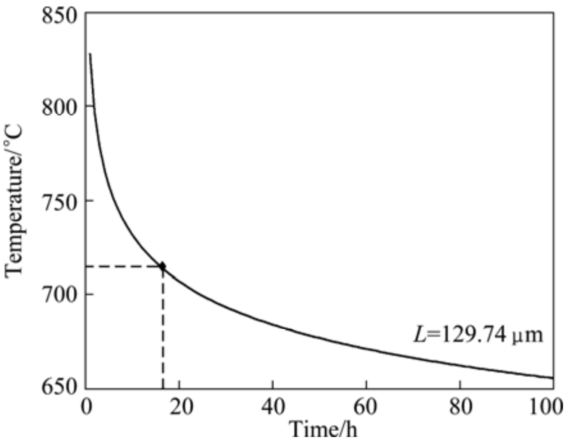

Fig. 11 Homogenization kinetics curve of Mn

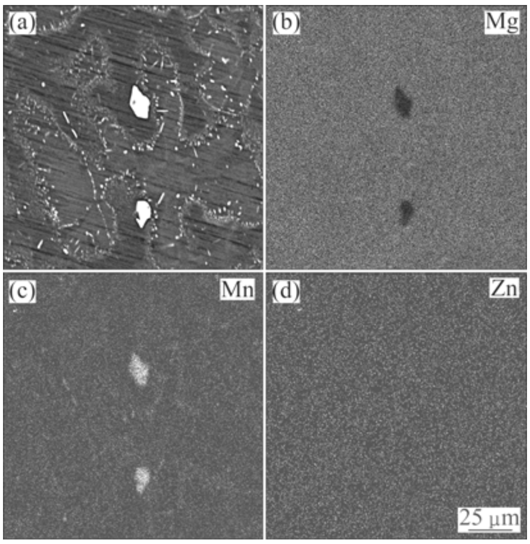

Fig. 12 Scanning electron microstructure and main elements distribution in homogenized alloy: (a) Backscattered electron image; (b) Element distribution of Mg; (c) Element distribution of Mn; (d) Element distribution of Zn

4 Conclusions

1) Serious dendritic segregation exists in the as-cast alloy. The main elements Mg, Mn and Zn are largely enriched in the grain boundaries. The dissolvable interdendritic phases in as-cast alloy consist of Zn, Cu-contained $\beta(Al_3Mg_2)$ phase, Fe-rich Al_6Mn and AlMgSi phase.

2) By increasing the homogenization temperature or prolonging the holding time, the residual phases are dissolved into the matrix gradually, grain boundaries become sparse and the distribution of all the elements becomes more homogenized, which can be described by a constitutive equation in exponential function.

3) The overburnt temperature of 5059 alloy is 460 °C. And the suitable homogenization treatment is at 450 °C for 24 h, which is consistent with the result of homogenizing kinetic analysis. In the aluminum matrix, fine $\beta(Al_3Mg_2)$ particles and rod-like Al_6Mn particles are evenly dispersed in it.

References

[1] European Aluminum Association. Aluminum in commercial vehicles [M]. Brussels: European Aluminum Association, 2011: 44−49.

[2] LEE Sheng-Long, WU Shinn-Tyan. Influence of soaking treatments on hot ductility of Al−4.85pct Mg alloys containing Mn [J]. Metallurgical Transactions A, 1986, 17(5): 833−841.

[3] KANNAN K, VETRANO J S, HAMITON C H. Effects of alloy modification and thermomechanical processing on recrystallization of Al−Mn−Mg alloys [J]. Metallurgical and Materials Transactions A, 1996, 27(10): 2947−2957.

[4] RAYNAUD G M, GOMIERO P. The potential of 5383 alloy in marine applications [C]//Proceedings of Alumitech'97. Atlanta: Aluminum Association, Inc, 1997: 353−66.

[5] DURAN A, DIF R. New alloy development at pechiney: A new generation of 5383 [C]//WILSON P A, HEARN G E. Conf Proc FAST 2001, vol. 3. Southampton: Southampton University, 2001: 223−230.

[6] WU L M, WANG W H, HSUB Y F, TRONG S. Effects of homogenization treatment on recrystallization behavior and dispersoid distribution in an Al−Zn−Mg−Sc−Zr alloy [J]. Journal of Alloys and Compounds, 2008, 456(1−2): 163−169.

[7] HE Zhen-bo, YAN Yan, ZHONG Shen, ZHENG Zi-qiao. Effect of aging treatments on microstructure and corrosion behavior of 7A55 alloy plate [J]. The Chinese Journal of Nonferrous Metals, 2010, 20(12): 2291−2297. (in Chinese)

[8] LIU Xiao-yan, PAN Qing-lin, FAN Xi, HE Yun-bin, LI Wen-bin, LIANG Wen-jie. Microstructural evolution of Al−Cu−Mg−Ag alloy during homogenization [J]. Journal of Alloys and Compounds, 2009, 484(1−2): 790−794.

[9] WANG Guo-jun, XIONG Bai-qing, ZHANG Yong-an, LI Zhi-hui, LI Pei-yue. Microstructural characterization of as-cast and homogenized 2D70 aluminum alloy [J]. International Journal of Minerals, Metallurgy and Materials, 2009, 16(4): 427−431.

[10] DU Zhi-ming, CHEN Gang, HAN Fei, CAO Guang-xiang, LIU Jun, LI Hong-wei, ZHANG Xin, XIE Shui-sheng. Homogenization on microstructure and mechanical properties of 2A50 aluminum alloy prepared by liquid forging [J]. Transactions of Nonferrous Metals Society of China, 2011, 21(11): 2384−2390.

[11] LI Wen-bin, PAN Qing-lin, XIAO Yan-ping, HE Yun-bin, LIU Xiao-yan. Microstructural evolution of ultra-high strength Al−Zn−Cu−Mg−Zr alloy containing Sc during homogenization [J]. Transactions of Nonferrous Metals Society of China, 2011, 21(10): 2127−2133.

[12] HUSKINS E L, CAO B, RAMESH K T. Strengthening mechanisms in an Al−Mg alloy [J]. Materials Science and Engineering A, 2010, 527(6): 1292−1298.

[13] HE L Z, LI X H, LIU X T, WANG X J, ZHANG H T, CUI J Z. Effects of homogenization microstructures and properties of a new type Al−Mg−Mn−Zr−Ti−Er alloy [J]. Materials Science and Engineering A, 2010, 527(29−30): 7510−7518.

[14] KAIBYSHEV R, MUSIN F, AVTOKRATOVA E, MOTOHASKI Y. Deformation behavior of a modified 5083 aluminum alloy [J]. Materials Science and Engineering A, 2005, 392: 373−379.
[15] LEE Shih-Wei, YEH Jien-Wei. Superplasticity of 5083 alloys with Zr and Mn additions produced by reciprocating extrusion [J]. Materials Science and Engineering A, 2007, 460−461: 409−419.
[16] KAIBYSHEV R, MUSIN F, LESUER D R, NIEH T G. Superplastic behavior of an Al−Mg alloy at elevated temperatures [J]. Materials Science and Engineering A, 2003, 342(1−2): 169−177.
[17] SHEWMAN P G. Diffusion in solids [M]. New York: Mc-Graw-Hill, 1963: 61.
[18] DU Yong, CHANG Y A, HUANG Bai-yun, GONG Wei-ping, JIN Zhan-peng, XU Hong-hui, YUAN Zhao-hui, LIU Yong, HE Yue-hui, XIE F Y. Diffusion coefficients of some solutes in FCC and liquid Al: Critical evaluation and correlation [J]. Materials Science and Engineering A, 2003, 363(1−2): 140−151.

5059 铝合金均匀化金属间相的演变

蒋海春[1,2]，叶凌英[1,2]，张新明[1,2]，顾 刚[1,2]，张 盼[1,2]，吴豫陇[1,2]

1. 中南大学 材料科学与工程学院，长沙 410083；
2. 中南大学 有色金属材料科学与工程教育部重点实验室，长沙 410083

摘 要：利用光学显微镜(OM)、扫描电子显微镜(SEM)、透射电镜(TEM)、能谱分析(EDS)、差示扫描量热法(DSC)、X 射线衍射(XRD)等手段研究了 5059 铝合金均匀化热处理过程中金属间相的演变。结果表明：5059 铝合金铸锭中枝晶偏析严重，大量难溶金属间相在晶界处呈连续网状分布。难溶金属间相由富含 Zn、Cu 元素的非平衡 $\beta(Al_3Mg_2)$相、Fe 元素富集的 Al_6Mn 共晶相以及 Mg_2Si 平衡相组成。在均匀化热处理过程中，难溶金属间相发生回溶，并析出大量弥散的 $\beta(Al_3Mg_2)$相和短棒状的 Al_6Mn 粒子。根据实验观测及均匀化动力学方程计算结果，得到合金的最佳均匀化热处理制度为(450 °C，24 h)。

关键词：金属间相；5059 铝合金；均匀化热处理；显微组织；演变

(Edited by Hua YANG)